NASA TM X-386

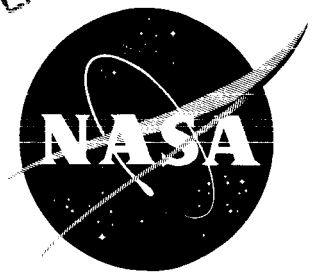

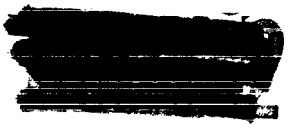

NASA TM X-386

TECHNICAL MEMORANDUM

X-386

EFFECTS OF BOATTAILED AFTERBODIES ON BASE HEATING AND MOTOR AERODYNAMIC HINGE MOMENTS OF A ROCKET MISSILE

By Robert A. Wasko

Lewis Research Center
Cleveland, Ohio

NATIONAL AERONAUTICS AND SPACE ADMINISTRATION

WASHINGTON

September 1960

NATIONAL AERONAUTICS AND SPACE ADMINISTRATION

TECHNICAL MEMORANDUM X-386

EFFECTS OF BOATTAILED AFTERBODIES ON BASE HEATING AND MOTOR AERODYNAMIC HINGE MOMENTS OF A ROCKET MISSILE*

By Robert A. Wasko

SUMMARY

Base-region temperatures and rocket hinge moments were investigated for simulated missiles with boattailed afterbodies in the 8- by 6-foot wind tunnel of the Lewis Research Center.

The basic model was a wing-supported body, approximately 8 inches in diameter, housing a 1000-pound-thrust rocket motor which used JP-4 fuel and liquid oxygen as propellants and extended approximately 0.32 body diameter beyond the base.

Tests were conducted over a Mach number range of 0.8 to 2.0 for a nominal rocket chamber pressure of 500 pounds per square inch absolute, motor gimbal angles of 0 and -4°, and a range of angle of attack and oxidant-fuel ratio.

There was no base heating for any afterbody configuration through the entire range of variables. Data presented in NASA TM X-82 indicate that a straight open-base afterbody with the same rocket extension had base temperatures as high as 1000° F above tunnel stagnation temperature. However, for both boattail configurations, a distinct pressure rise occurred on the rocket external surface near the exit plane. This resulted in rocket hinge moments for all conditions of nonzero angle of attack and/or motor gimbal.

INTRODUCTION

It has been observed in both flight measurements and wind-tunnel studies that at transonic and supersonic speeds rocket missiles can suffer a base temperature rise due to entrainment and afterburning of jet gases in the base region. An analysis of the interactions between the jet exhaust and the free stream presented in reference 1 shows that the entrainment of jet gases is a result of the inability of a portion of the gases in the boundary of the wake formed by the jet mixing zone to negotiate the wake pressure rise and the consequent recirculation of these gases into the base region.

*Title, Unclassified.

One method of eliminating the base temperature rise, as reported in reference 2, is to eliminate the jet mixing zone as a boundary of the wake by extending the nozzle beyond the base until the wake pressure rise begins to appear on the motor. However, the extended nozzles were subjected to asymmetric external pressures by motor gimbal and angle of attack which resulted in forces on the nozzle structure.

In the investigation of reference 3, the use of bleed scoops eliminated entrainment of jet gases, and at least for one configuration, did not result in additional motor forces. The engine compartment could be subjected to a temperature rise due to ram compression at higher supersonic Mach numbers.

Another technique, which conceivably could be used to prevent entrainment of jet gases, is to boattail the afterbody. The stream air would thus follow the boattail contour and impinge on the motor provided that the boattail angles were not so large as to lead to boattail flow separation. Impingement of the free stream on the motor would lead to the external forces on the motor that occurred with the extended nozzles.

This report presents the results of a brief study in the 8- by 6-foot supersonic wind tunnel of the base-region temperatures and pressures for a rocket missile model having boattailed afterbodies. Two boattails of 11° and 15° angles alternately replaced the straight afterbody of reference 2. The rocket motor had a nozzle with an area ratio of 8, used liquid oxygen and JP-4 fuel as propellants, and operated at a nominal chamber pressure of 500 pounds per square inch absolute. Test variables included oxidant-fuel ratio, model angle of attack, and rocket gimbal angle at Mach numbers of 0.8, 1.4, and 2.0.

APPARATUS AND PROCEDURE

A simulated ballistic missile approximately 80 inches long and 8 inches in diameter, having a cone-ogive nose and two interchangeable boattailed afterbodies, was wing mounted in the 8- by 6-foot wind tunnel of the Lewis Research Center as shown in figures 1 and 2.

The rocket motor used in this test had a thrust of 1000 pounds, was water-cooled, and used liquid oxygen and JP-4 fuel as propellants. The motor could be gimballed to 4° in the pitch plane about a point located 7.25 inches upstream of the rocket exit plane. It was essentially the same as the engine used for the investigation reported in reference 2. In an effort to obtain data which could be correlated with the straight-afterbody data of reference 2, a rocket extension of 2.53 inches (0.32 body diameter) was used. The rocket nozzle was contoured as shown in figure 1 and had a jet-exit to throat area ratio of 8.

Two open-base afterbodies of 11° and 15° boattail angle were used. Design and instrumentation details are shown in figure 3. The 11° boattail angle was the minimum angle allowed by model geometry for maintaining a rocket extension of 2.53 inches and providing sufficient clearance at the base for motor gimbal requirements. The 15° boattail angle was considered the maximum angle to avoid separation of the boattail flow. It was anticipated that for both boattails the flow would impinge on the motor.

Each boattail was instrumented with Chromel-Alumel thermocouples in the engine compartment and on the base of the afterbody. Radial temperature profiles 1/2 inch downstream of the base were measured with a rake of five equispaced thermocouples.

Base pressure was measured by four equispaced static-pressure orifices. External static-pressure distributions on the top and bottom of the rocket nozzle were obtained by means of static-pressure orifices distributed as shown in figure 3. The combustion chamber was instrumented with a static-pressure orifice for monitoring and recording combustion-chamber pressure.

The rocket engine was operated over an oxidant-fuel-ratio range of approximately 1.5 to 2.8 at a combustion-chamber pressure of 500 pounds per square inch absolute. Based on nominal values of free-stream static pressure, the ratio of chamber pressure to free-stream static pressure P_c/p_0 was 159, 90, and 47 for free-stream Mach numbers of 2.0, 1.4, and 0.8, respectively.

The procedure for rocket ignition and operation and the procedure and method of monitoring and recording the data are identical with those of reference 2 and are presented in detail therein. All temperatures and pressures presented herein are for steady-state conditions.

RESULTS AND DISCUSSION

Base-Region Temperature

The effect of oxidant-fuel ratio on engine-compartment, base, and rake temperatures for the 11° and 15° boattails is shown in figure 4. The ordinate of the plot is an incremental temperature defined as $\Delta T = T_{max} - T_0$, where T_{max} represents the maximum value of the temperature at each of the measuring stations. (Symbols are defined in the appendix.)

For both configurations temperatures at all measuring stations were within 40° F of tunnel stagnation temperatures for all Mach numbers. Average stagnation temperatures were 200°, 160°, and 140° F

at Mach numbers of 2.0, 1.4, and 0.8, respectively. Angle of attack and motor gimbal angle had no effect on base-region temperatures. Data presented in reference 2 indicate that a straight open-base afterbody with the same rocket extension experienced base temperatures as high as 1000° F above tunnel stagnation values.

Base Pressures

Base pressure ratio is presented in figure 5 as a function of jet-exit to free-stream static-pressure ratio. Both with the jet on and off base pressures for these boattailed afterbodies were generally higher than base pressures for a blunt-base afterbody configuration having the same extension ratio as well as larger extensions (see figs. 11(a) to (c) of ref. 2). In addition, there was a significant increase in boattail base pressure from jet off to jet on in contradistinction to straight-afterbody configurations (ref. 2), which at these same jet pressure ratios showed little change in base pressure.

Rocket-Motor External Pressures

Distributions of jet-on motor external pressure are presented in figure 6(a) for the missile and motor in a neutral attitude (α, 0; β, 0). The anticipated pressure rise due to free-stream impingement on the motor was present at all Mach numbers for both boattails and generally occurred approximately 1.5 inches upstream of the rocket exit plane. A blunt-base afterbody with the same rocket extension did not indicate a pressure rise on the motor at any Mach number (fig. 12(a), ref. 2).

The effect of motor gimbal angle (α, 0; β, -4°) on external pressure distribution is shown in figure 6(b). For a negative gimbal angle achieved by pitching the nozzle upward about the gimbal point, there exists a significant pressure asymmetry between top and bottom surfaces. Furthermore, for the top surfaces the pressure rise was farther upstream and higher than for the no-gimbal condition (β, 0) shown in figure 6(a). Data not presented show that a pressure-distribution asymmetry of smaller magnitude exists when the missile is at an angle of attack (β, 0; α, -5°).

Moments about the motor gimbal point were computed from the motor external pressure. At each orifice station (see fig. 3) a linear circumferential pressure distribution was assumed between top and bottom orifices. A normal force per unit axial length was then determined at each station. A positive moment is defined as that which tends to pitch the missile nose up.

Because of fabrication tolerances, both boattails were geometrically asymmetrical. As a result of this and motor misalinement with the model centerline, hinge moments existed when the missile and motor were in a neutral position.

The moment data presented in figure 7 in the form of motor moment coefficient C_m as a function of Mach number are corrected for this error. At each Mach number, the moment coefficient computed for a condition of zero angle of attack and zero angle of gimbal was considered a "tare" moment coefficient. The data presented then are the actual moment coefficient computed minus the tare moment coefficient at that Mach number.

The effect of motor gimbal angle (α, 0; β, -4°) on C_m is shown in figure 7(a); the effect of angle of attack (α, -5°; β, 0) on C_m is shown in figure 7(b). A negative motor gimbal angle resulted in positive moments, while a negative angle of attack resulted in negative moments.

The combined effect of gimbal angle and angle of attack on C_m is shown in figure 7(c). It appears that the positive moments from motor gimbal counteract the negative values from angle of attack, since the resulting hinge moments are approximately the algebraic sum of those in figures 7(a) and (b).

For comparison, data are shown in figures 7(a) and (c) for a straight afterbody with a 0.59 extension ratio that were obtained from figure 17 of reference 3 at the condition of zero metered base-bleed flow. In general, the moment coefficients for the straight afterbody and a 0.59 extension were less than those for the 11° boattail motor. For $\alpha = -5^\circ$ and $\beta = -4^\circ$, the coefficient for the 0.59 motor extension reversed sign, unlike the boattail motor moment coefficient. Base-region temperatures for the 0.59 extension, as reported in reference 2, were slightly greater than the boattail base temperatures.

The data for a straight afterbody with a 0.78 extension ratio were obtained from reference 2. For $\alpha = 0$ and $\beta = -4^\circ$ at Mach 2.0, the motor moment coefficient for the 0.78 extension was greater than the 11° boattail motor moment coefficient, and at $\alpha = -5^\circ$, $\beta = -4^\circ$ reversed sign as did C_m for the 0.59 extension, but was negatively larger than the latter. Base temperatures for the 0.78 extension reported in reference 2 are of the same magnitude as boattail base temperatures.

Neither this investigation nor the investigations of the straight afterbodies (refs. 2 and 3) determined an optimum design from the viewpoint of low base temperature with minimum external motor moments;

therefore, the relative merits of boattail configurations and straight afterbodies with varying rocket extension ratios cannot be evaluated from figure 7 and the preceding comments. Rather, for any of these afterbody configurations (except base-bleed-flow configurations) low base temperatures are concomitant with motor hinge moments.

SUMMARY OF RESULTS

The study of boattail afterbody effects on base heating and rocket hinge moments using a liquid-oxygen - JP-4 fuel rocket motor at Mach numbers of 0.8, 1.4, and 2.0 indicated the following:

1. Base-region temperatures were of the order of tunnel stagnation temperature through the entire range of test variables.

2. The boattailed afterbodies of this study resulted in a distinct pressure rise on the motor due to free-stream impingement which led to motor hinge moments.

Lewis Research Center
National Aeronautics and Space Administration
Cleveland, Ohio, June 21, 1960

APPENDIX - SYMBOLS

A	area
C_m	engine aerodynamic moment coefficient, $m/qA_e l$
D	diameter
l	distance from engine gimbal point to nozzle exit plane, 7.25 in.
M	Mach number
m	engine aerodynamic moment about gimbal point due to engine external pressure
P	total pressure
p	static pressure
q	dynamic pressure
T	total temperature
α	**model angle of attack**
β	**rocket engine gimbal angle**

Subscripts:

b	base
c	combustion chamber
e	rocket exit plane
l	local external pressure on rocket motor
max	maximum
t	rocket nozzle throat
0	free-stream conditions

REFERENCES

1. Baughman, L. Eugene, Kochendorfer, Fred D.: Jet Effects on Base Pressures of Conical Afterbodies at Mach 1.91 and 3.12. NASA RM E57E06, 1957.

2. Chiccine, Bruce G., Valerino, Alfred S., and Shinn, Arthur M.: Experimental Investigation of Base Heating and Rocket Hinge Moments for a Simulated Missile Through a Mach Number Range of 0.8 to 2.0. NASA TM X-82, 1959.

3. Valerino, Alfred S., Shinn, Arthur M., Jr., and Chiccine, Bruce G.: Effects of Base Bleed Flow on Base Region Temperatures and Pressures of Several Simulated Missile Afterbody Configurations - Mach Number Range of 0.8 to 2.0. NASA TM X-153, 1960.

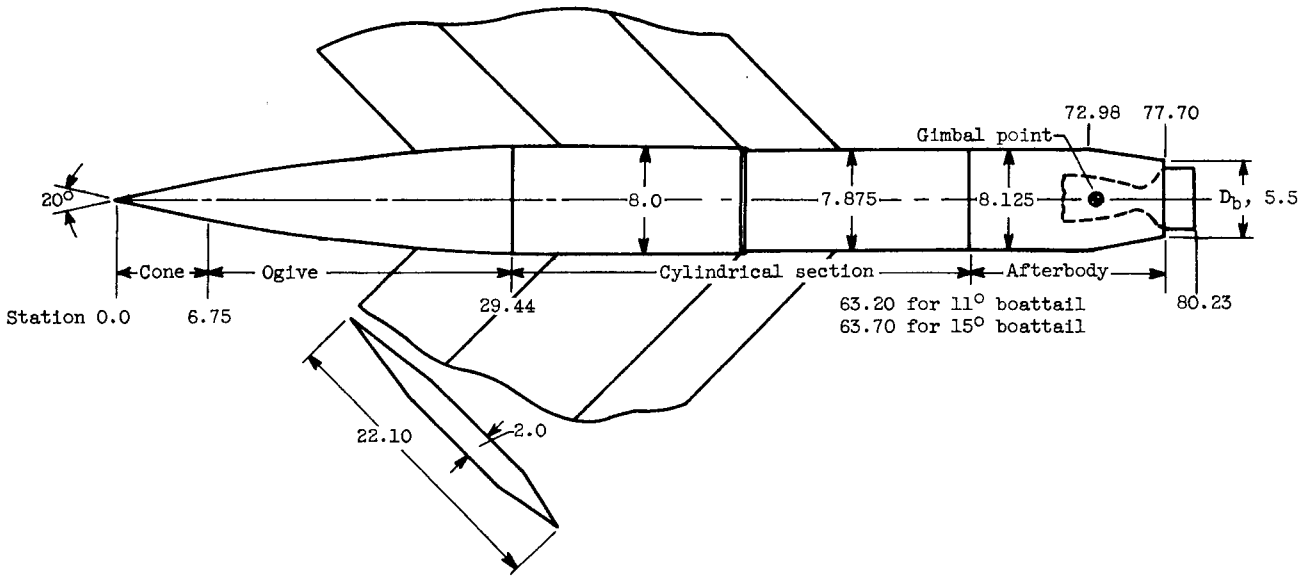

(a) Model assembly.

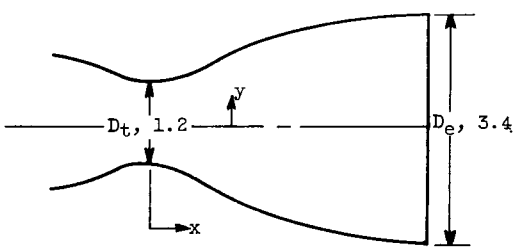

x	y
0	0.600
.090	.617
.275	.691
.609	.826
.944	.960
1.322	1.109
1.669	1.233
1.968	1.328
2.408	1.450
2.756	1.530
3.048	1.450
2.756	1.530
3.048	1.591
3.343	1.639
3.581	1.665
3.819	1.683
4.057	1.698
4.132	1.700

(b) Internal nozzle contour.

Figure 1. - Schematic drawing of model. (Dimensions are in inches.)

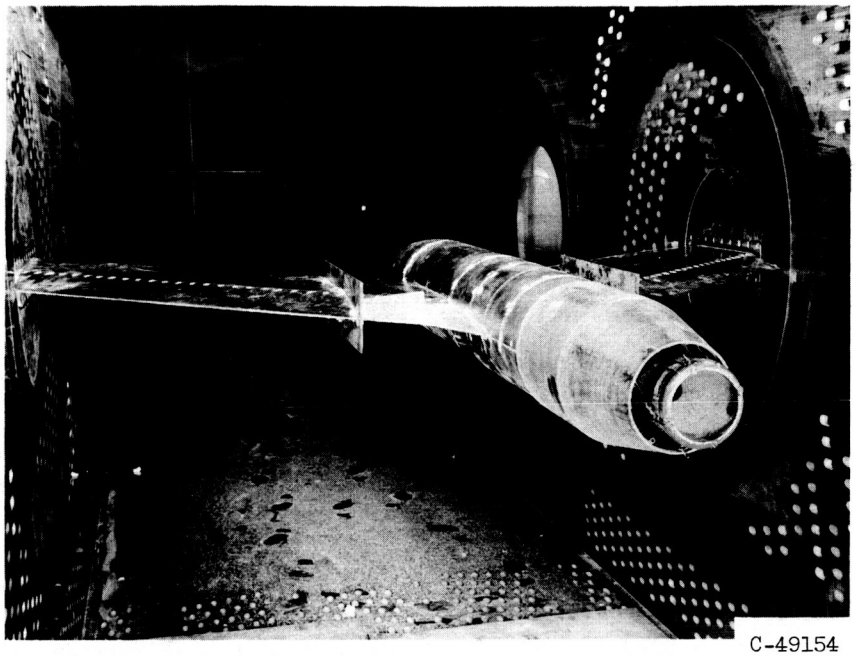

C-49154

(a) Model mounted in tunnel test section.

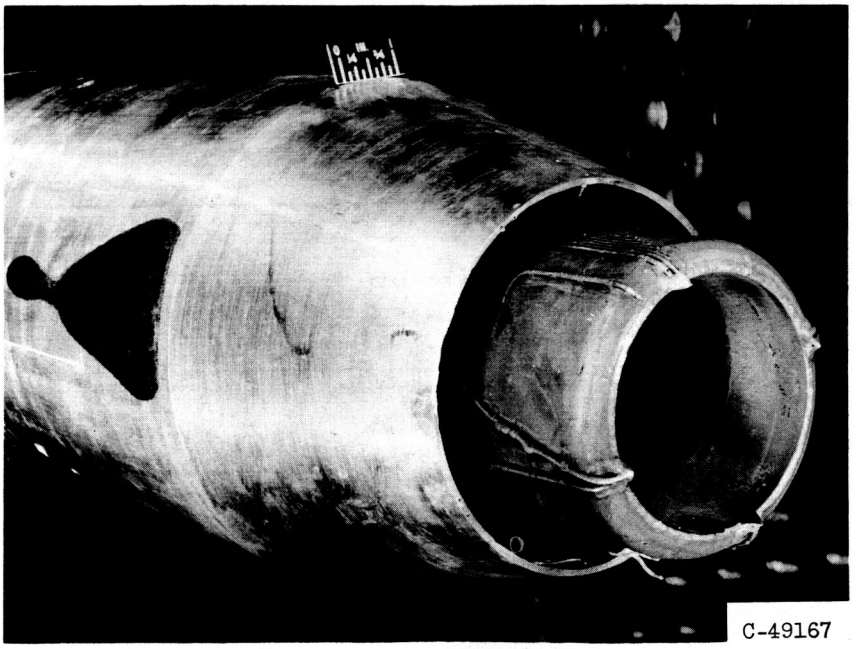

C-49167

(b) 15° Boattailed afterbody.

Figure 2. - Model photographs.

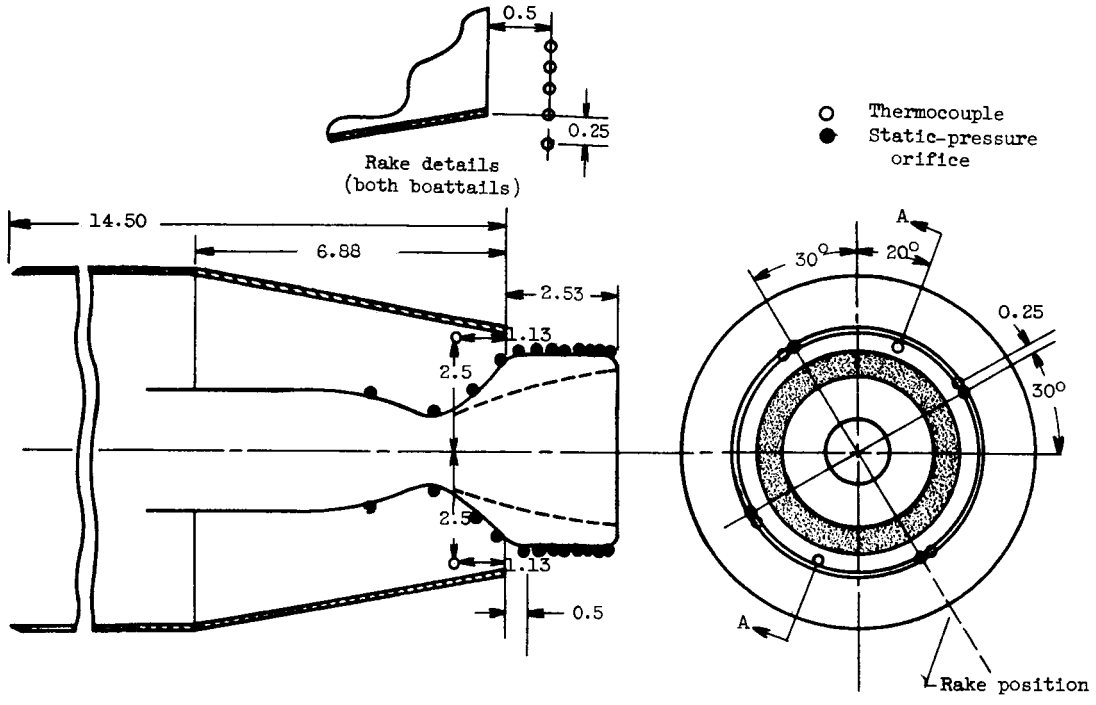

(a) 11° Boattail.

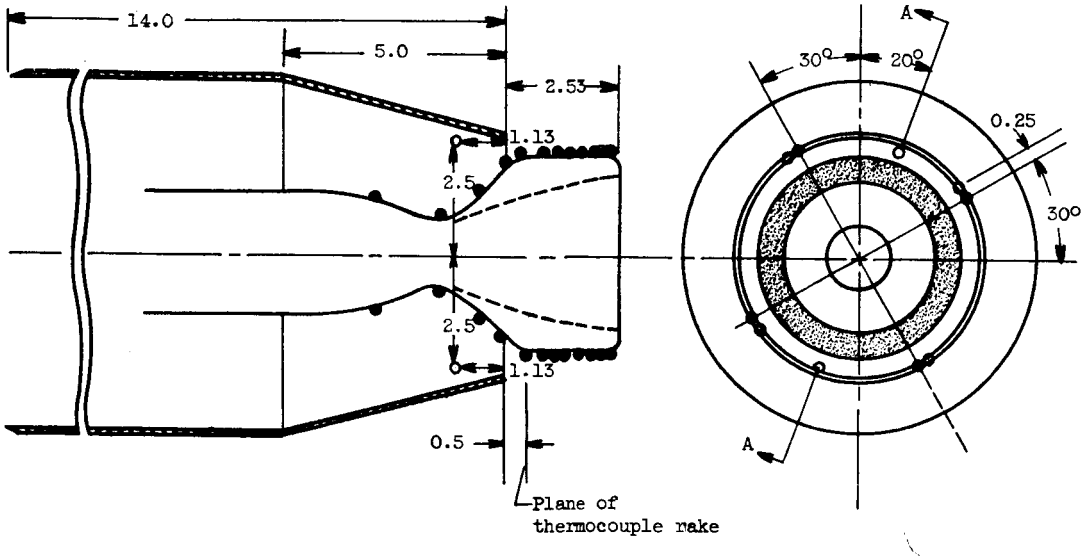

(b) 15° Boattail.

Figure 3. - Afterbody and motor geometry and thermocouple and pressure instrumentation locations. (Dimensions are in inches.)

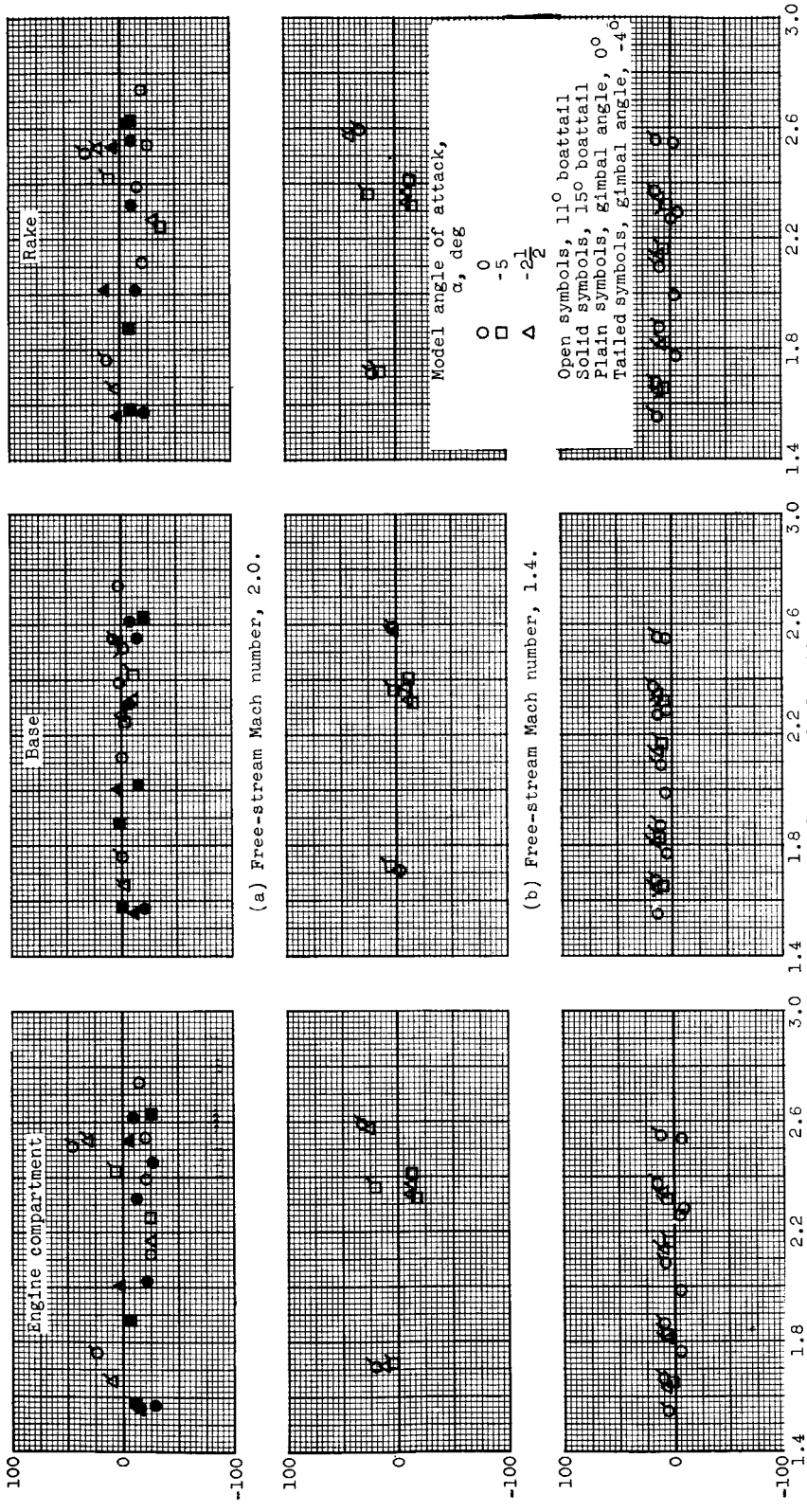

(a) Free-stream Mach number, 2.0.

(b) Free-stream Mach number, 1.4.

(c) Free-stream Mach number, 0.8.

Figure 4. - Effect of oxidant-fuel ratio on base-region temperatures.

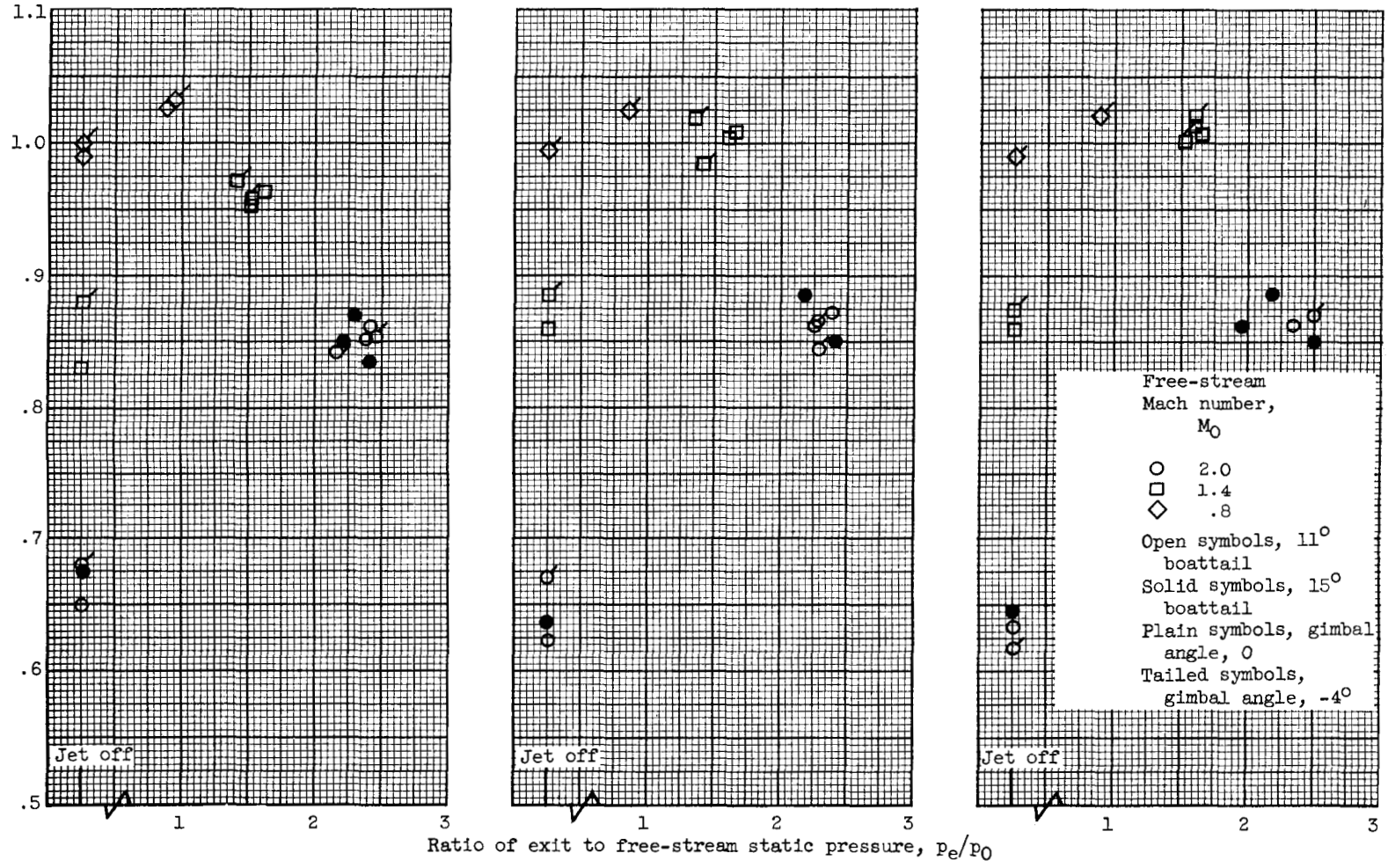

(a) Model angle of attack, α, 0. (b) Model angle of attack, α, $-2\frac{1}{2}^\circ$. (c) Model angle of attack, α, -5°.

Figure 5. - Effect of jet-exit static-pressure ratio on base pressure.

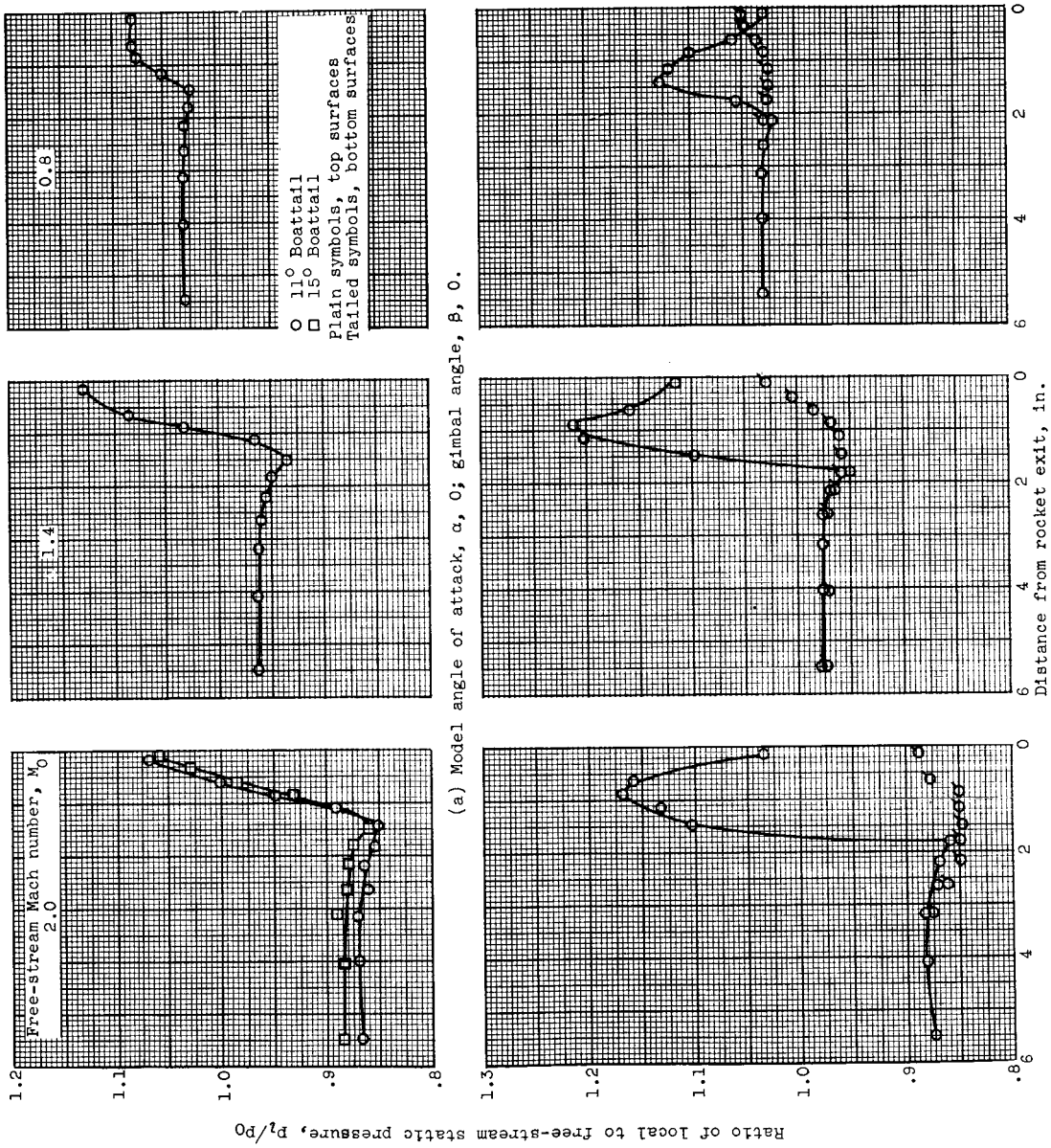

(a) Model angle of attack, α, 0; gimbal angle, β, 0.

(b) Model angle of attack, α, 0; gimbal angle, β, -4°.

Figure 6. - Distribution of motor external pressure with jet on.

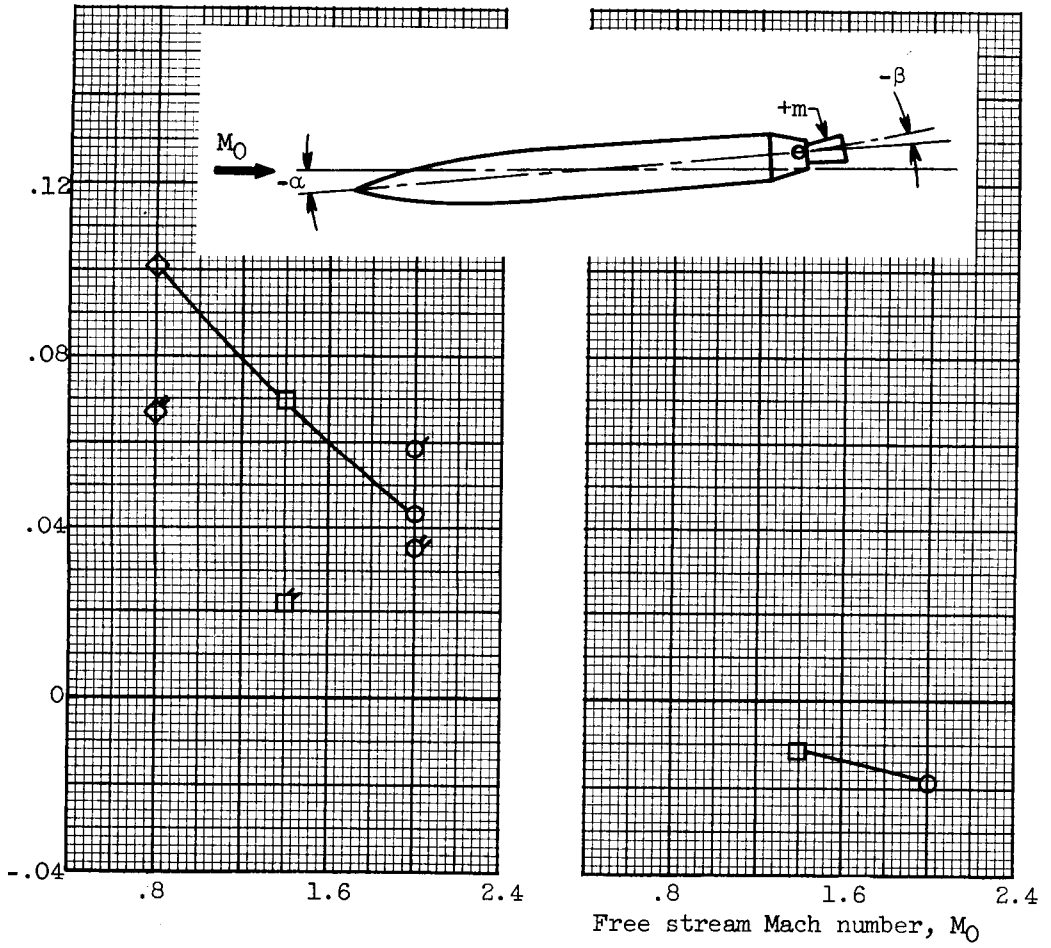

(a) Model angle of attack, α, 0; gimbal angle, β, -4°.

(b) Model angle of attack, α, -5°; gimbal angle, β, 0.

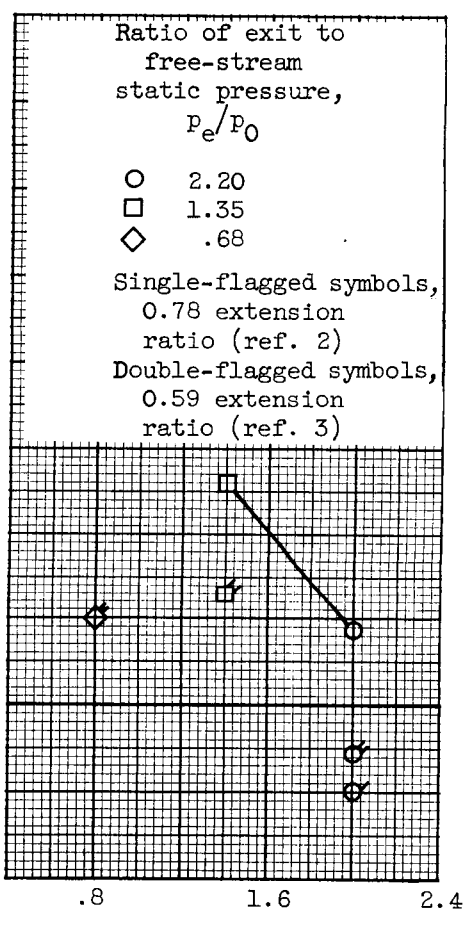

(c) Model angle of attack, α, -5°; gimbal angle, β, -4°.

Figure 7. - Motor aerodynamic moment coefficient for 11° boattail.